Annals of Pure and Applied Mathematics
Vol. 3, No. 1, 2013, 27-40
ISSN: 2279-087X (P), 2279-0888(online)
Published on 16 May 2013
www.researchmathsci.org

Annals of
Pure and Applied
Mathematics

Effect of Reynolds Number on Aerodynamic Characteristics of an Airfoil with Flap

[1] ***Md. Hasanuzzaman*** **and** [2] ***Mohammad Mashud***

[1] Department of Mathematics and [2] Department of Mechanical Engineering
Khulna University of Engineering & Technology
Khulna-9203, Bangladesh
Email: mdmashud@yahoo.com

Received 17 April 2013; accepted 25April 2013

Abstract. Over the past few decades due to rapid growth of computer uses and it's calculation capability it has been adopted to solve numerical problem by many CFD softwere. By solving Numerical problem thorugh CFD quite accurate and precious result may obtain than laboratory test which is quite expensive. That's why before work with new design firstly it was tested by numarical method throgh available CFD softwere in computer and based on the result best design is choose to undergo for laboratory test. This reduce time and cost. The goal of this project is to familiar with FLUENT CFD softwere and it's application. After study flow character stics for varrying Reynolds noumber for an airfoil with and without flap was invistigated. Flow characterstics in terms pressre co-efficient, velocity vector and pressure distribution was observed for varrying Reynolds number. When air flow over airfoil shock wave is formed on it's upper surface and flow is separated at trailing edge due to adverse pressure gradient. Numerical modelling of 2-D Airfoil without flap and with flap was designed in GAMBIT tool in FLUENT. In this case boundary condition also implimented. Then flow characterstics for designed aifoil was investigated and it is shown graphically at solution steps along with lift and drag plot against angle of attack.

Keywords: Aerodynamic, Airfoil with Flap

AMS Mathematics Subject Classification (2010): 76D99, 76E09

1. Introduction

An airfoil is the croos sectional shape of an airplane wing. When airfoil moved through a fluid such as air produces an aerodynamic force. The component of this force perpendicular to the direction of motion is called lift. The component parallel to the direction of motion is called drag. The lift on an airfoil is primarily the result of its angle of attack and shape. When oriented at a suitable angle, the airfoil deflects the oncoming air, resulting in a force on the airfoil in the direction opposite to the deflection. This force is known as aerodynamic force and can be resolved into two components: Lift and drag. Most airfoil shapes require a positive angle of attack to generate lift, but cambered

airfoils can generate lift at zero angle of attack. This "turning" of the air in the vicinity of the airfoil creates curved streamlines which results in lower pressure on one side and higher pressure on the other. This pressure difference is accompanied by a velocity difference, via Bernoulli's principle, so the resulting flow field about the airfoil has a higher average velocity on the upper surface than on the lower surface. The lift force can be related directly to the average top/bottom velocity difference without computing.

The pressure by using the concept of circulation and the Kutta-Joukowski theorem [1, 2, 3, 4]. As wing is combination of large number of airfoil, so when air flows over airplane wing it causes airplane to lift. Wing should be proper shape for smooth lift. That's why airfoil size and shape playing an important role on airplane flying. Plenty of experience was done on effective airfoil design and still it's modification work is going on. Basic element of an airfoil is shown in Figure 1.

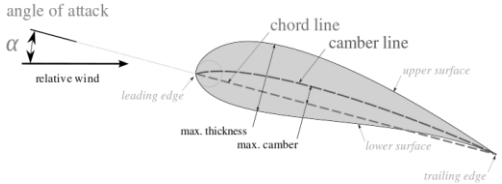

Figure 1: Basic elements of an airfoil

When airfoil moves through air, boundary of air is formed on airfoil surface. Due to presence of friction in air flow causes shear stress at airfoil surface which slow down the air flow near the surface: in the presence of an adverse pressure gradient, there will be a tendency for the boundary layer to separate from the surface. This adverse pressure gradient on top of the airfoil becomes stronger by increase in angle of attack. At stall angle the flow is separated from the upper surface. When the boundary layer separates, its displacement thickness increases sharply, this modifies the outside potential flow and pressure field. In the case of airfoils, the pressure field modification results in an increase in pressure drag and increase loss of lift, all of which are undesirable. So it is desirable to delay the flow separation. The objective of the flow control is to manipulate a particular flow field with a small energy input typically aiming to increase the lift and reduce the drag, to enhance the mixture of momentum, energy, and species, and to suppress the flow-induced noise [5]. The performance and stability of an airplane is often degraded by flow separation. Traditionally, flow separation control is implemented through airfoil shaping, leading edge slat, surface cooling, moving walls, tripping early transition to turbulence, and near-wall momentum addition. Among the near-wall momentum addition methods, steady or pulsed blowing jets and vortex generators (VG) have been widely used [6].

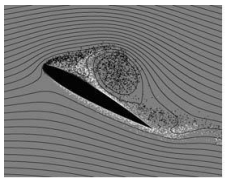

Figure 2: Flow separation on airfoil

In recent years,control devices involving zero-net-mass-flux oscillatory jets or synthetic jets have shown good feasibility for industrial applications and effectiveness in controlling flow separation (Glezer & Amitay 2002; Rumsey et al. 2004; Wygnanski 2004) [7]. From previous experimen it is found that synthetic jet and forcing/non-forcing (oscillatory/steady) suction/blowing on the aerofoil leading edge can increase lift and decrease drag [8]. The application of synthetic jets to flow separation control isbased on their ability to stabilize the boundary layer by adding/removing momentum to/from the boundary layer with the formation of vortical structures. It has been observed that relatively large quantities of steady blowing near the point of separation can re-attach the flow and increase the lift, but the steady blowing may also cause a thickening of both the boundary layer and the wake behind the airfoil which leads to increased drag (Nagib et al, 2001). The experiments conducted by Bons et al. (Bons et al, 2001). [6] have shown that steady Vortex Generator Jets (VGJ) have the effect of reducing or entirely eliminating the separation zone on the suction surface of the airfoil at low Reynolds number, while the pulsed VGJs produce a comparable improvement to that for steady VGJs but with an order of magnitude less required mass-flow [9]. In simple terms a vortex generator is a device that creates a swirl or vortex of fluid due to it's shape. A great deal of research has been done to develop guidelines to determine the size and shape of a proper vortex generator.Vortex generators work by mixing high energy air from the free stream with the lower energy air found in the boundary layer. The vortices created by these generators cascades energy and momentum from the free stream to the boundary layer due to their recirculatory motion. In other words, the vortex generator increases the mean stream wise momentum of the boundary layer by drawing in high momentum fluid from the frees stream. This process is called re-energizing the boundary layer. The higher energy fluid is more resistant to separation and allows higher performance of the airfoil.Separation control is a broad and widely studied topic, and thorough reviews on its various applications have been published (Gad-el-Hak and Bushnell 1991, Greenblatt and Wygnanski 2000). Passive separation control techniques that generally constitute geometric changes such as vortex generators and slotted flaps/slats are employed on many operational aircraft. These control elements are effective if the aircraft is operating in a flight regime that is in their design envelope. However, in off design conditions, passive control elements can have detrimental effects that are often manifested in the form of increased drag. Despite this drawback, the benefits of passive control techniques often out weight the incurred cost created by their application to the aerodynamic surface. Active separation control has gained popularity in recent years due to its potential for maintaining or enhancing the benefits of passive control techniques without the penalty associated with operation in off design conditions. The main difference here is that active control can be turned on and off by command allowing additional flexibility. Active control strategies also have the potential to be implemented in a feedback system that coupled with adequate sensors and controller could create even greater benefits in flight efficiency and maneuver ability. A complete review of active separation control is a subject in itself. Rather, the following background information focuses on separation control studies that examine the effect of two dimensional actuation on two dimensional airfoil models. Technological advances over the last few decades have allowed researchers to more fully explore the wide parameters pace associated with this research topic. Accordingly, significant advances in the understanding of separated flow

phenomena in response to actuation have followed. Among the most widely accepted is that unsteady actuation via pulsed blowing, pulsed suction or both (zero net mass flux) is more effective than steady forcing (Seifert et al. 1996). The range of effective dimensionless frequencies associated with this is on the order of unity for which the dimensionless frequency (reduced frequency or Strouhal number), F^+, is defined as $F^+ = fx_{sp}/U_\infty$ where f is the forcing frequency, x_{sp} is the length of the separated region and U_∞ is the free stream velocity (Darabi and Wygnanski 2004, Glezer et al. 2005). This parameter under scores the importance of the characteristic length scale of separated flow phenomena, x_{sp},which is the length of the separation zone over the body in question (Seifert et al. 1996). Physically, the reduced frequency of unity requires that a perturbation must be introduced during the time that the free stream flow propagates over the separated region. The importance of actuator location is closely related to this expression since the shear layer created between the freestream and the low-speed separated region by nature selectively amplifies small perturbations if these are introduced near its receptivity region. The optimum choice of this location for unsteady actuation is generally at or slightly upstream of the separation point. This ensures that the shear layer is excited by the control perturbations near its receptivity point. Successful introduction of such forcing creates large span wise vortices that develop via the Kelvin–Helmholtz instability. These vortices encourage momentum transport between the free stream and the separated region thus reattaching the flow (Darabi and Wygnanski 2004, Melton et al. 2005). Forcing at higher frequencies ($F^+>10$) has been classified as a different regime and is characterized by enhanced energy dissipation associated with spatial scales in the boundary layer (Amitay and Glezer 2002). Studies on control of trailing edge separation have shown that significantly more momentum in put is required incomparison with leading edge contro (Melton et al. 2006). This is commensurate with the existence of a thicker, likely turbulent boundary layer that develops along the main element of the airfoil. Such results also support leading edge separation control findings that show greater centripetal acceleration created by airfoil surface curvature requires additional momentum for realizing similar control authority (Greenblatt and Wygnanski 2003). Because of these challanges, it is difficult to fully attach the flow over the trailing edge flap. Consequently, both experimental and numerical studies show that lift gains associated with this are often manifested from upstream effects such as an increase in over all circulation (Kiedaisch et al. 2006, Melton et al. 2006). Additional work has shown that the simultaneous use of multiple actuators distributed along the airfoil chord has been more successful than the contribution from each actuator alone (Greenblatt 2007). Not surprisingly, the relative phase between actuator input signals is an important parameter that is highly dependent on the spacing of the actuators, the excitation frequency and the velocity just external to the boundary layer (Greenblatt 2007, Melton et al. 2007).

2. Separation control with DBD plasma actuators

The recent interest in plasma actuators for aerodynamic flow control is motivated by their simple construction, lack of moving parts, high band width and ease of implementation. Because of these amenable characteristics, researchers have investigated their application in a variety of flow control problems particularly those associated with flow separation. These studies and the current state of the DBD plasma knowledge base are summarized in various review articles (Moreau 2007, Corke et al. 2009). While such devices are

relatively new to the aerodynamic community, DBD plasma actuators have long been used in a variety of industrial applications such as ozone generation (Kogelschatz 2003). The use of DBD plasma actuators for airfoil separation control at locations other than the leading edge has been limited. Studies have reported that actuators placed near the trailing edge of airfoils can produce effects similar to plain flaps with deflections of a few degrees (Vorobiev et al. 2008). This results in a uniform increase in lift coefficient across all angles of attack and a slight reduction in minimum drag coefficient, C_D, at Reynolds numbers on the order of 105 corresponding to velocities of a few tens of meters per second (He et al. 2009). To date, DBD plasma actuators have not produced sufficient momentum to eliminate separation for flows over simpled eflected flaps at Re *105* unless the free stream velocity is quite low (Mabe et al. 2009). The mechanism responsible for separation control by DBD plasma is most often associated with the wall jet generation described earlier, but whether this results in boundary layer tripping, energizing or amplification of instabilities is still in debate and depends on the flow system under consideration. For separation control explicitly, the state of the boundary layer (laminar or turbulent) just upstream of the actuator will also play a role. Unlike traditional unsteady jets created with voice coils or piezo-ceramic disks, the exact location at which the plasma actuator accomplishes control is not immediately obvious, but actuators placed at or slightly upstream of the separation location give favorable results (Huang et al. 2006, Sosa et al. 2007, Jolibois et al. 2008). This appears consistent with modeling results that's how the highest force density associated with such devices is near the edge of the exposed electrode (Enloe et al. 2004, Corke et al. 2007). Like synthetics jets, AC driven DBD plasma actuators are often most effective for separation control and lift enhancement when excitation is created with reduced frequency (F^+) on the order of unity (Huang et al. 2006, Greenblatt et al. 2008, Patel et al. 2008, Benard et al. 2009). To operate in this fashion, the actuator must be excited with a sufficiently high carrier frequency to produce the plasma (*1–10*kHz) and modulated at a lower frequency to excite the long wave leng thin stabilities associated with most separated flow dynamics. This behavior is analogous to synthetic jets created by piezoelectric diaphragms at produce the highest intensity fluctuations when excited near the resonant frequency of the disk and/or cavity that is often on the order of a few kHz. Many studies of separation control with DBD plasma actuators assume that the flow does not feel perturbations created by the high-frequency carrier signal. For the majority of low speed applications, this is true because the instabilities involved are not receptive to high-frequency perturbations and instead feel their effect as a quasi-steady phenomenon. However, it has been confirmed that the movement of charged species in the plasma does infact create a perturbation at the frequency of plasma generation and thus suggests the possibility of using of DBD plasma actuators for high frequency forcing applications if sufficient amplitude can be produced (Takeuchi et al. 2007, Boucinha et al. 2008). It has been shown that the force production of AC driven DBD plasma actuators is dependent on the oxygen content, ambient pressure and humidity of the environment (Kim et al. 2007, Abe et al. 2008, Benard et al. 2009a). This makes the application of such devices at cruising altitudes in working flight environments questionable at this time. Never the less, strides continue to be made for DBD plasma implementation as they have been used with varying degrees of success in feedback control and flight testing (Patel et al. 2007, Sidorenko et al. 2008). Even more promising is ongoing research for improved methods of generating DBD

plasma actuation that rely on nano second pulses (Likhanskii et al. 2007, Opaits et al. 2007). These wave forms seem to accomplish control based on thermal effects alone similar to arc filament based plasma actuators (Samimy et al. 2007) and have demonstrated leading edge airfoil separation control authority upto Mach *0.85* (Roupassov et al. 2009) .Because of the amenable characteristics outlined earlier and the variety of parameters that can be explored, plasma actuators continue to be an emphasized point of research in aerospace applications [10].

Another methods of controlling flow separation on high-lift airfoils utilize multi-element flaps that allow mixing of fluid between the pressure and suction sides. Experiments on using flaps at trailing edge shows that as angle between flap and airfoil increases airfoil stall condition also delayed that means flow is controlled.

The objective of this current work is to determine the aerodynamic characterstics for varrying Reynolds number over an airfoil using flap at upper surface by CFD solver. In this experiment NACA 2415 airfoil and FLUENT CFD softwere are used.

Figure 3: Airfoil NACA 2415

Figure 4: Airfoil NACA 2415 with flap

3. Mathematical Modeling

Two equation turbulence models are one of the most common types of turbulence models. Models like the k-epsilon and the k-omega model have become industry standard models and are commonly used for most types of engineering problems. Two equation turbulence models are also very much still an active area of research and new refined two-equation models are still being developed. By definition, two equation models include two extra transport equations to represent the turbulent properties of the flow. This allows a two equation models to account for history effects like convection and diffusion of turbulence energy [11]. Most often one of the transported variables is the turbulent kinetic energy k. The second variable varies depending on what type of two-equation model it is. Common choices are the turbulent dissipation $\in$, or the specific dissipation ω. The second variable can be thought of as the variable that determines the scale of the turbulence (length-scale or time-scale), whereas the first variable k, determines the energy in the turbulence. There are two major formulations of k-epsilon models. The original impetus for the k-epsilon model was to improve the mixing-length model, as well as to find an alternative to algebraically prescribing turbulent length scales in moderate to high complexity flows. The k-epsilon model has been shown to be useful for free-shear layer flows with relatively small pressure gradients. Similarly, for wall-bounded and internal flows, the model gives good results only in cases where mean pressure gradients are small; accuracy has been shown experimentally to be reduced for flows containing large adverse pressure gradients. One might infer then, that the K-epsilon model would be an inappropriate choice for problems such as inlets and compressors.

The k-$\in$ model introduces two new variables into the system of equations.

To solve this problem numerically following equation are used by FLUENT CFD software.

$$\mathrm{Re} = \frac{\rho v c}{\mu} \tag{1}$$

Continuity equation:

Conservation form

$$\frac{\delta \rho}{\delta t} + \nabla . (\rho V) = 0 \tag{2}$$

Equation (2) is partial differential equation form of the continuity equation. It was derived on the basis on of an infinitesimally small element fixed in space. The infinitesimally small aspect of the element is why the equation is obtained directly in partial differential form.

Momentum equation:

Navier stocks equation

$$\frac{\partial(\rho u)}{\partial t} + \frac{\partial(\rho u^2)}{\partial x} + \frac{\partial(\rho uv)}{\partial y} = -\frac{\partial p}{\partial x} + \frac{\partial}{\partial x}(\lambda \nabla . V + 2\mu \frac{\partial u}{\partial x}) + \frac{\partial}{\partial y}[\mu (\frac{\partial v}{\partial x} + \frac{\partial u}{\partial y})] + \rho F(x) \tag{3a}$$

$$\frac{\partial(\rho v)}{\partial t} + \frac{\partial(\rho v^2)}{\partial y} + \frac{\partial(\rho uv)}{\partial x} = -\frac{\partial p}{\partial y} + \frac{\partial}{\partial y}(\lambda \nabla . V + 2\mu \frac{\partial v}{\partial y}) + \frac{\partial}{\partial x}[\mu(\frac{\partial v}{\partial x} + \frac{\partial u}{\partial y})] + \rho F(y) \tag{3b}$$

Equation of state:
The classic equation of state for an ideal gas,

$$\mathbf{p = \rho R T} \tag{4}$$

Turbulence modeling:

Transport equations for standard k-epsilon model
For turbulent kinetic energy k

$$\frac{\partial}{\partial t}(\rho k) + \frac{\partial}{\partial x_i}(\rho k u_i) = \frac{\partial}{\partial x_j}[(\mu + \frac{\mu_t}{\sigma_k})\frac{\partial k}{\partial x_j}] + P_k + P_b - \rho \in -Y_M + S_k \tag{5}$$

For dissipation $\in$

$$\frac{\partial}{\partial t}(\rho \in) + \frac{\partial}{\partial x_i}(\rho \in u_i) = \frac{\partial}{\partial x_j}[(\mu + \frac{\mu_t}{\sigma_\in})\frac{\partial \in}{\partial x_j}] + C_{1\in}\frac{\in}{k}(P_k + C_{3\in}P_b) - C_{2\in}\rho\frac{\in^2}{k} + S_\in \tag{6}$$

$$\text{where } C_1 = \max[0.43, \frac{\eta}{\eta+5}], \quad \eta = S\frac{k}{\in}, \quad S = \sqrt{2S_{ij}S_{ij}} \tag{7}$$

In these equations, P_k represents the generation of turbulence kinetic energy due to the mean velocity gradients, calculated in same manner as standard k-epsilon model. P_b is the generation of turbulence kinetic energy due to buoyancy, calculated in same way as standard k-epsilon model.

Modelling Turbulent Viscosity is

$$\mu_t = \rho C_\mu \frac{k^2}{\in} \tag{8}$$

where

$$C_\mu = \frac{1}{A_0 + A_s \frac{kU^*}{\in}}, \quad U^* \equiv \sqrt{S_{ij}S_{ij} + \tilde{\Omega}_{ij}\tilde{\Omega}_{ij}}$$

$$\tilde{\Omega}_{ij} = \Omega_{ij} - 2 \in_{ijk} \omega_{ij}, \quad \Omega_{ij} = \overline{\Omega}_{ij} - \in_{ijk} \omega_{ij}$$

and $\overline{\Omega}_{ij}$ is the mean rate-of-rotation tensor viewed in a rotating reference frame with angular velocity ω_k.

The model constants A_0 and A_s are given by $A_0 = 4.04, \quad A_s = \sqrt{6}\cos\phi$

$$\phi = \frac{1}{3}\cos^{-1}(\sqrt{6}W), \; W = \frac{S_{ij}S_{jk}S_{ki}}{\tilde{S}^3}, \; \tilde{S} = \sqrt{S_{ij}S_{ij}}, \; S_{ij} = \frac{1}{2}(\frac{\partial u_j}{\partial x_i} + \frac{\partial u_i}{\partial x_j}) \tag{9}$$

where the model constants are $C_{1\in} = 1.44$, $C_2 = 1.9$, $\sigma_k = 1.0$, $\sigma_\in = 1.2$ (10)

4. Numerical Modelling

The solution method utilized for the simulation had a pressure based solver with implicit formulation, 2-D domain geometry, absolute velocity formulation, and superficial velocity for porous formulation. For this test, a simple solver and an external compressible flow model for the turbulence was utilized. The green-gauss cell based was used for the gradient option. There are different equations used for flow and turbulence. A simple method was used for the pressure-velocity coupling. For the discrimination, a standard pressure was used and simulations are 5m/sec and turbulence viscosity ratio is 10. A fully turbulent flow solution was used in ANSYS fluent 6.3.26, where realizable k-$\in$ model was used for turbulent viscosity. A simple solver was utilized for the simulation.

5. Computational Domain

NACA 2415 airfoil was used to run this experiment which chord(c) length is *1*m. As flow over airfoil is external flow, so we have defined a Fairfield boundary and mesh the region

between the airfoil geometry and the Fairfield boundary. The Fairfield region is created by following measurement:

Label	X	Y	Z
A	1	12.5	0
B	21	12.5	0
C	21	0	0
D	21	-12.5	0
E	1	-12.5	0
F	-11.5	0	0
G	1	0	0

Flow characteristics was determined for given input velocity *4*m/s, *5*m/s, *6*m/s for no flap condition and with flap of *0.15* m long and *0.02*m width at7^0at maximum camber position. Successive grid length was *0.96*c at all side. Computational domain is divided into *4*zones. Ferfield-*1*, Ferfield-*2*, Ferfield-*3* and Airfoil.

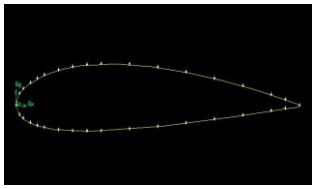

Figure 5: geometry of Airfoil withoutflap

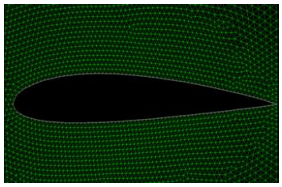

Figure 6: Grid for airfoil without flap

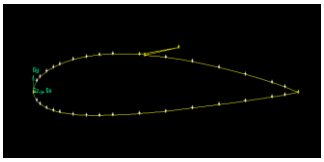

Figure 7: geometry of Airfoil with flap

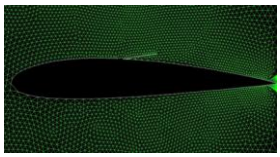

Figure 8: Grid for Airfoil with flap

The computational domain was created with 5 face zones and 86460 nodes. The domain is divided in four parts for applying the boundary conditions. These are the airfoil section, farfield 1, farfield 2, and farfield 3. For the airfoil section the solid wall no slip condition was applied. For the farfield 1 boundary condition was velocity inlet and for other two farfields pressure outlet was selected as the boundary condition. The boundary condition for farfield was applied as the velocity components. For X component velocity was applied as $5\cos\alpha$ as α is the angle of attack. For Y component of velocity $5\sin\alpha$ is applied. For the design, mesh generation and applying the boundary condition to the domain to be calculated Gambit was used and Fluent was used as the solver. Fluent has a reliable computational accuracy for fluid flow arrangements and holds good results.

For five different flap arrangement the design was created in Gambit and the mesh was created as per the spoiler position. Around the airfoil section the mesh was fine enough to observe the velocity and pressure contour perfectly. The effect of the spoiler on pressure distribution of airfoil surface can be observed simultaneously as the computation for each angle of attack is done. The grid generated was checked before the

computation started and there was a satisfactory output for grid checking for every spoiler position. Convergence criteria were selected as 10^{-3}. This indicates the value taken as the result was constant for consecutive 1000 iterations. Other criterions like continuity residuals were also monitored.

6. Result and Discussion

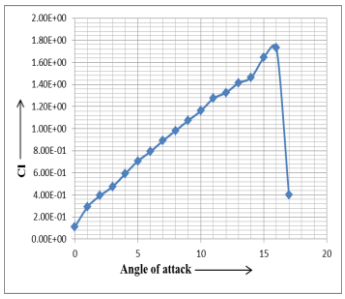

Figure 9: Lift curve for airfoil without flap

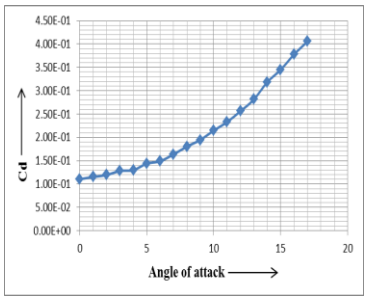

Figure 10: Drag curve for airfoil without flap

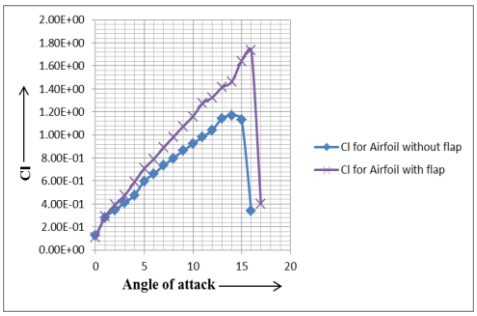

Figure 11: Comparisn of Cl vs angle of atack for Airfoil with and without flap for velocity 4 m/s

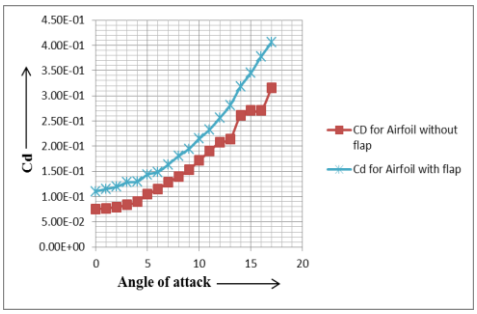

Figure 12: Comparisn of Cd vs angle of attack for Airfoil with and without flap for velocity 4 m/s

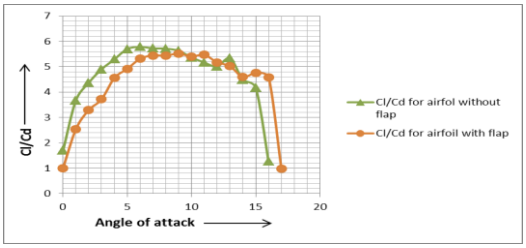

Figure 13: Comparison of Cl/Cd vs angle of attack for Airfoil with and without flap for velocity 4 m/s

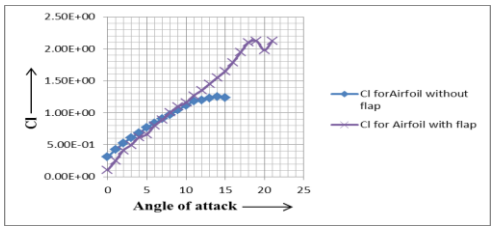

Figure 14: Comparisn of Cl vs angle of attack for Aitfoil with and without flap for velocity 5 m/s

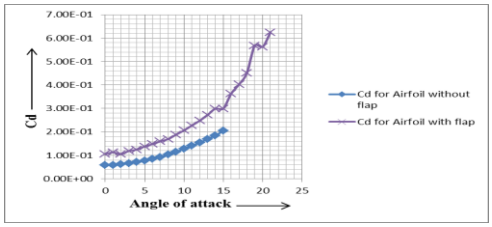

Figure 15: Comparisn of Cd vs angle of attack for Aitfoil with and without flap for velocity 5 m/s

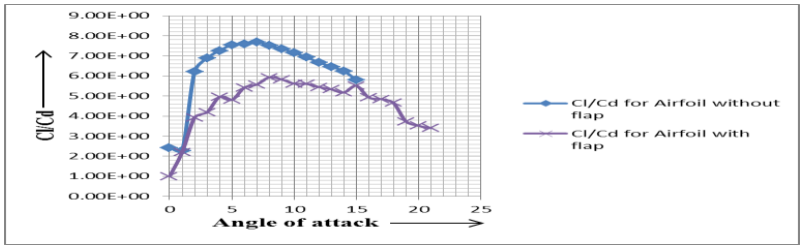

Figure 16: Comparisn of Cl/Cd vs angle of attack for Airfoil with and witout flap for velocity 5 m/s

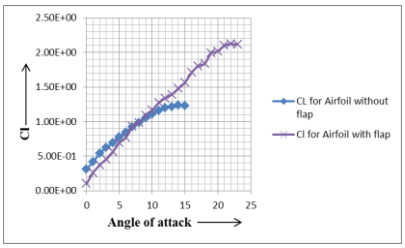

Figure 17: Comparisn of Cl vs angle of attack for Airfoil withouit flap and with flap for velocity 6 m/s

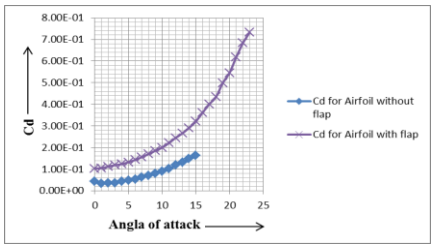

Figure 18: Comparisn of Cd vs angle of attack for Airfoil withouit flap and with flap for velocity 6 m/s

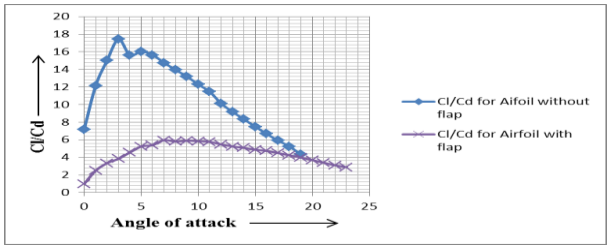

Figure 19: Comparisn of Cl/Cd vs angle of attack for Airfoil with and without flap for velocity 6 m/s

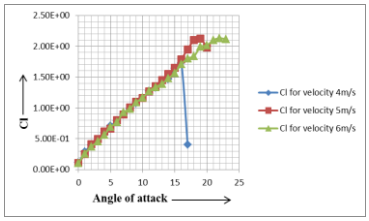

Figure 20: Comparison plot for Cl vs angle of attck for varying velocity

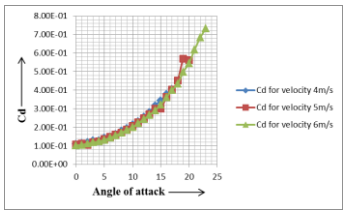

Figure 21: Comparison plot for Cd vs angle of attack for varying velocity

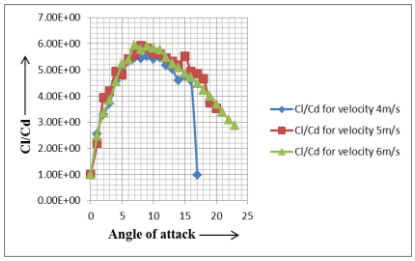

Figure 22: Comparison plot for Cl/Cd vs angle of attack for varying velocity

From above figures it's clear that for varying inlet velocity from *4*m/s to 6m/s have shown typical results of Reynolds number effects on lift distribution on airfoil. It's not difficult to say that as increase in Reynolds number improve the lift and drag characterstics in whole. Form comparison plot for any certain velocity it is seen that lift for airfoil with flap is started incresing from begaing than from no flap condition and drag for flap is always more that without flap. Presence of flap also cause increse of stall angle from no flap condition for a difinite velocity. It has seen that increase of velocity has no effect on stall angle for no flap condition except lift, which is increase as increase in velocity. Different characterstics is visualize from comparison plot for airfoil with flap that increase in vlocity increases lift as well as stall angle. After complete solution of NACA2415 airfoil with flap in FLUENT resultant characterstics plot shows the effect of Reynolds number on pressure distribution on airfoil, the training-edge pressure coefficient and pressure gradient along wall direction which suggests shock wave location and intensity. It can be seen that the upper surface pressure distribution including the location and intensity of shock wave and trailing-edge pressure coefficient, changed apparently with variable Reynolds numbers, while the lower surface pressure distribution is not so sensitive to the Reynolds number. As the Reynolds number increases, the boundary layer of upper surface gets thinner, the location of shock wave moves afterward, intensity of shock wave increases, trailing-edge pressure coefficient improves. From valocity vector and contours of static pressure distribution it's seen that due to presence of flap flow separats from the surface but reattach with the surface after crossing the flap. As angle of attack increases the possition of reattaching point moves to forward. It's also seen that at stall condition position of reattaching point moves to left as increase of velocity. This cause increase in lift and delay in flow separation. Thus from

results obtained by numerical solution shows that presence of flap increase lift and delay the stall condition which is the basic condition for contrilling flow separation.

Contour of velocity magnitude and static pressure:

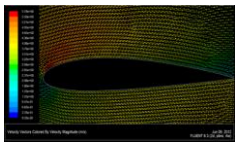

Figure 23: Contour of velocity magnitude for $\alpha = 14^0$

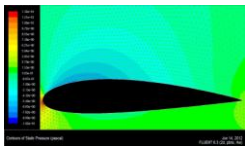

Figure 24: Contours of static pressure for $\alpha = 14^0$

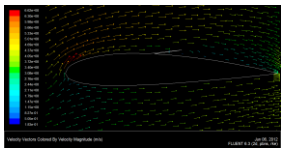

Figure 25: Contour of velocity magnitude for $\alpha = 14^0$

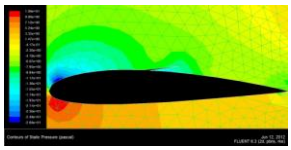

Figure 26: Contours of static pressure for $\alpha = 14^0$

Contour of the velocity magnitude and static pressure for airfoil without flap for angle 14^0 are shown in the Figures 23 and 24. The effect of the flap is shown by the velocity and the static pressure contour at angle of attact 15 in the Figures 25 and 26. They are the indicate of the changes that occur during the flow over an airfoil section with flap. It is seen that the air flow behind the flap is being disturbed. As the angle of attack increases the region of the negative pressure tends towards the leadind edge and the pressure difference is decreased. Thus the lift force fot the airfoil without any flap is higher than that of the airfoil having a flap. Also the flap resists the flow of the air passing the airfoil, which causes the drag force to be increased.

7. Conclusion

The main objective of this project is to sudy FLUENT CFD softwere and to see effect of reynolds number on aerodynamic characterstics of an airfoil with flap by using this softwere. FLUENT softwere is studied very well including it's all function and application. From numarical study of arifoil NACA 2415 in FLUENT softwere it's seen that flow separation can be controle by using flap at maximum camber position.

REFERENCES

1. Halliday, David and Resnick, Robert, *Fundamentals of Physics, 3rd edition*, John Wiley & Sons.
2. NASA Glenn Research Center, Archived from the original on 5 July 2011, Retrieved *2011-06-29.*
3. Weltner, Klaus, Ingelman-Sundberg, Martin, *Physics of Flight - reviewed*

4. Babinsky, Holger (November 2003), How do wings work.
5. M. Serdar Genc, Ünver Kaynak, Control of Laminar Separation Bubble over a NACA 2415 Aerofoil at Low Re Transitional Flow Using Blowing/Suction, 13th International Conference on Aerospace Sciences and Aviation Technology, ASAT-13, May 26–28, 2009, Paper: ASAT-13-AE-11.
6. Hua Shan, Li Jiang and Chaoqun Liu, Numerical study of passive and active flow separation control over a NACA0012 airfoil, University of Texas at Arlington, Arlington TX 76019, 2007.
7. D.You and P.Moin, Study of flow separation over an airfoil with synthetic jet control using large-eddy simulation, Center for Turbulence Research Annual Research Briefs 2007.
8. M. Serdar Genc and Ünver Kaynak, Control of laminar separation bubble over a NACA2415 aerofoil at low re transitional flow using blowing/suction, 13th International Conference on Aerospace Sciences and Aviation Technology, ASAT-13, May 26–28, 2009, Paper: ASAT-13-AE-11.
9. Shutian Deng, Li Jiang and Chaoqun Liu, DNS for flow separation control around airfoil by steady and pulsed jets, Department of Mathematics, University of Texas at Arlington, Arlington, TX 76016, USA, Paper presented at the RTO AVT Specialists' Meeting on "Enhancement of NATO Military Flight Vehicle Performance by Management of Interacting Boundary Layer Transition and Separation", held in Prague, Czech Republic, 4-7 October 2004, and published in RTO-MP-AVT-111.
10. JesseLittle, Munetake Nishihara, Igor Adamovich and Mo Samimy, High-lift airfoil trailing edge separation control using a single dielectric barrier discharge plasma actuator, *Exp Fluids*, *48* (2010), 521–537, DOI10.1007/s00348-009-0755-x, Springer-Verlag 2009.
11. Standard k-epsilon model, *CFD-Wiki, the free CFD reference*.
12. James E. Fitzpatrick and G. Chested, Furlong-effect of spoiler types lateral-control devices on the TWBTING moments of a wing of NACA 230-series Airfoil Sections-Langle Memorial Aeronautical Laboratory, Langley Field, VA.
13. *Airfoil-CFD-Wiki, the free reference.*